Estimation of nocturnal CO_2 and N_2O soil emissions from changes in surface boundary layer mass storage

Richard H. Grant[1], Rex A. Omonode[1]

[1] Department of Agronomy, Purdue University, West Lafayette, Indiana, 47907, USA

Correspondence to: Richard H. Grant (rgrant@purdue.edu)

Abstract. Annual budgets of greenhouse and other trace gases requires knowledge of the emissions throughout the year. Unfortunately emissions into the surface boundary layer during stable, calm nocturnal periods are not measureable using most micrometeorological methods due to non-stationarity and uncoupled flow. However, during nocturnal periods with very light winds carbon dioxide (CO_2) and nitrous oxide (N_2O) frequently accumulates near the surface and this mass accumulation can be used to determine emissions. Gas concentrations were measured at four heights (one within and three above canopy) and turbulence was measured at three heights above a mature 2.5 m high maize canopy from 23 July to 10 September 2015. Nocturnal CO_2 and N_2O fluxes from the canopy were determined using the accumulation of mass within a 6.3 m high control volume and out the top of the control volume within the nocturnal surface boundary layer. Diffusive fluxes were estimated by flux gradient method. The total accumulative and diffusive fluxes during near-calm nights (friction velocities < 0.05 ms^{-1}) averaged 1.16 μmol $m^{-2}s^{-1}$ CO_2 and 0.53 nmol $m^{-2}s^{-1}$ N_2O. Fluxes were also measured using chambers. Daily mean CO_2 flux determined by the accumulation method were 90% to 130% of those determined using soil chambers. Daily mean N_2O flux determined by the accumulation method were 60% to 80% of that determined using soil chambers. The better signal to noise ratio of the chamber method for CO_2 over N_2O, non-stationary flow, assumed Schmidt numbers and anemometer tilt were likely contributing reasons for the differences in chambers versus accumulated nocturnal mass flux estimates. Near-surface N_2O accumulative flux measurements in more homogeneous regions and with greater depth are needed to confirm the conclusion that mass accumulation can be effectively used to estimate soil emissions during nearly calm nights.

1 Introduction

Evaluation of the annual emissions of greenhouse and other trace gases emitted from agricultural fields and landscapes requires knowledge of the emissions during representative periods of the year. Micrometeorological methods are widely used to evaluate the emissions and uptake of carbon dioxide (CO_2) and to a lesser degree nitrous oxide (N_2O). The micrometeorological methods of eddy covariance, eddy diffusion, or Eulerian or Lagrangian dispersion however cannot be used to determine the exchange during stable, calm nocturnal periods due to lack of steady winds and turbulence characteristics assumptions (Pattey, et al, 2002). Due to the non-stationary winds, the integrated horizontal mass flux method is also limited to configurations in which the source area is enclosed or 'fenced' by profile measurements. Various efforts to estimate the exchange during these

periods have been devised- in some cases using purely statistical methods, some using empirical relationships, and some using alternative flux measurement methodologies (Aubinet et al, 2012). The primary difficulties of determining the flux in the surface boundary layer under stable nocturnal conditions include the possibility of advection, non-stationarity of the concentration and velocity fields, and the lack of a similarity theory to describe the non-stationary, intermittent exchange processes. A result of the negligible turbulent transport of mass away from the surface is a temporal change in storage of mass within a layer near the surface primarily a result of low vertical turbulent diffusion. This accumulation occurs initially in a shallow nocturnal surface boundary layer then through light continuous or intermittent turbulence deepens through a thicker (on the order of 100 m) stable nocturnal boundary layer (Kaimal and Finnigan, 1994). Xia et al (2011) noted an accumulation of ^{222}Rn within a 6.5 m deep surface boundary layer over a grass clearing of a forest preserve during nights with clear sky, light winds, and strong radiative cooling. Similar gas accumulations in the surface boundary layer at night have been conducted for CO_2, CH_4, and N_2O over pastures and crops (Pattey et al, 2002; Pendall et al., 2010). As weak turbulence mixes the surface boundary layer air with the cooling stable nocturnal boundary layer, gas mass accumulations become evident throughout much of the stable nocturnal boundary layer. Such mass accumulations are reported for CO_2, CH_4, and N_2O over crops, plantations, and forests (Pattey et al, 2002; Acevedo, et al., 2004; Acevedo, et al., 2008).

Using temporal mass accumulation for estimating flux under stable conditions assumes horizontal mass transport is negligible, there are no local sources of N_2O or CO_2 within the control volume, and that the exchange of mass between the control volume and the overlying air is minimal. If there is no flow in the surface boundary layer (SBL), then gases emitted from the soil surface will diffuse upward at roughly the rate of molecular diffusion (approx. 10^{-5} m^2s^{-1}). Such conditions are approximated in soil flux chambers but do not occur in the surface boundary layer beyond the laminar layer at the surface. Compared to the typical turbulent diffusion exchange coefficients, the molecular diffusion rate is negligible. Consequently gas diffusion from the surface is effectively stopped at any altitude were the diffusion rate decreases a few orders of magnitude. This provides the effective 'cap' on the mixing of gases in the control volume layer.

Many approaches have been used to define the conditions in which the accumulation of a gas as effectively capped in the surface boundary layer. Since the friction velocity (u_*) provides an index of turbulent mixing, Pattey et al (2002) used a u_* threshold for validating the quality of the 'cap'. Pendall et al (2010) defined the top of the accumulation control volume based on significant correlations between CO_2 (presumed from soil respiration) and CO, CH_4, N_2O, and H_2. The top of the control volume has been estimated by Acevedo et al (2004) using the top of an observed fog layer or the height of constant potential temperature and specific moisture in the early morning. Acevedo et al (2008) used the height of the strongest potential temperature inversion as the control volume top. Pattey et al (2002) determined the accumulation over the entire 10 m of profile measurements under constrained turbulent flow conditions. Using these 'cap' definitions, the temporal change in mass accumulations have been determined over relatively thin layers of air over crops (10 m thick; Pattey et al, 2002), pastures (5 m thick; Pendall et al., 2010) and plantations (8 m thick; Pendall et al., 2010). Other much thicker layers of at least 20 m have been defined over forests (Acevedo, et al., 2004; Acevedo, et al., 2008; Pendall et al., 2010).

The source area represented by a flux measurement (termed 'footprint') has a turbulent and advective component (Vesala et al, 2007) and depends on the height of the measurements, the duration of the averaging period used in the method, and the flow conditions during the measurements. The turbulent component to the flux footprint also cannot be readily assessed under these complex flow conditions since the determination of turbulent flux footprints depends on definable (stationary) flow (Vesala et al, 2007). Furthermore, the typical mass accumulation micrometeorological method integration period of at least an hour is typically longer than the averaging period of eddy covariance and most other micrometeorological flux measurement methods and hence less likely to be stationary flow throughout the period. If the flow were stationary, the longer integration period for the accumulation flux over other micrometeorological flux methods such as eddy covariance results in larger represented source areas for the measured flux than other micrometeorological flux measurements. Given the complex flow conditions of the stable nocturnal SBL (non-stationary flow and low turbulence), these longer integration intervals will result in an increased potential for advective mass contributions contributed to the SBL by nearby sources with differing emissions. Chambers et al (2011) attempted to determine the relative contribution of ^{222}Rn accumulation in the atmospheric boundary layer to a height of 50 m from mixing of local sources and that advected from 'remote' regions with greater or less soil flux using seasonal average HYSPLIT simulations (Draxler and Hess, 1998). Chambers et al (2011) found a frequent decoupling of flow between the 2 m and 50 m measurement heights during the night and suggested that the 50 m flow was in the residual layer and not the surface boundary layer. Such decoupling would not be simulated by HYSPLIT resulting in potentially significant errors in nocturnal surface boundary layer footprint determination. Furthermore, since HYSPLIT relies on well-defined turbulent characteristics to model the back-trajectory, the poorly defined non-stationary, intermittent flow of the nocturnal boundary layer cannot be well-represented in any HYSPLIT-based fetch estimate. Consequently estimates of the flux footprint during stable nocturnal conditions were not estimated by HYSPLIT but by assuming stationarity of hourly mean flow for 2 to 12 hours with footprint estimates driven by atmospheric motion in the daily, not turbulence time scales. These assumptions resulted in footprints extending 10 to 40 km away for winds averaging approximately 1.5 ms^{-1} (Chambers et al, 2011). Biraud et al (2002) estimated the fooprint for their ^{222}Rn flux estimates for the atmospheric boundary layer (ABL) based on sampling at 20 m and an assumed well-mixed ABL using HYSPLIT and assumed steady winds over the entire ABL for multiple days. They assumed the trajectory air parcel was in contact with the land if it was within 2 km above ground level (within the ABL). Consequently their footprint estimates were driven by atmospheric motion above the stable nocturnal surface boundary layer. As Chambers et al.(2011), Biraud et al (2002) assumed stationary flow conditions at all times and found wind speeds (at 10 m) ranging from 1.5 ms^{-1} to 8 ms^{-1} over four days corresponded to footprints extending 150 km to 200 km from the measurement location.

We evaluated the nocturnal flux of CO_2 and N_2O from maize-cropped land based on the temporal accumulation of mass storage within the surface boundary layer constrained vertically by the flow characteristics at the top of a layer 6.3 m deep.

2 Methods

N_2O and CO_2 fluxes were measured using three methods during the night between 2000 and 0400 local time (hereafter referred to as 20 h LT and 04 h LT) over nitrogen-fertilized fields during the summer of 2015. These fields are located in a relatively flat and homogeneous terrain (Fig. 1a) near West Lafayette, Indiana, USA (40.495° latitude and -86.994 ° longitude). The terrain rises to the north at a rate of only 2 m km^{-1} and land use is predominantly agricultural with cropped land covering 100% of the land within 1 km^2 and 97% of the within 10 km^2 (Table 1) and 83% within 25 km^2. Crops are generally alternating between maize and soybean with 83%, (1 km^2) 46% (10 km^2) and 40% (25 km^2) in maize in 2015.

The instrumented towers (described below) were situated in a tilled field ('200Sp'; Fig. 1b) in which 220 kg N ha^{-1} were applied as anhydrous ammonia (AA) at pre-plant in spring 2015. Three other fertilizer treatments were applied in fields near the towers: a 220 kg N ha^{-1} AA application on a no-till field ('200Fa; Fig. 1b), and a 110 kg N ha^{-1} AA application during the fall of 2014 followed by a pre-plant spring AA application of 110 kg N ha^{-1} ('100Fa/100Sp'; Fig. 1b) on a tilled (north) and no-till (south) field.

N_2O and CO_2 concentrations were measured from air sampled out of a 7 L min^{-1} air flow drawn from 1μm-filtered inlets at three heights: 2.8 m, 5 m, and 8 m above ground level (agl). Air was sampled sequentially for 5 minutes at each inlet. Mean concentrations were based on the last three of each five-minute interval to account for the time lag associated with the air flow and the measuring instruments. The 2.8 m point sample was made from a mast that was 18 m from the 5 and 8 m measurement mast (Fig. 1b). In addition a line sample based on a 50-m line with ten inlets drew air at 1 m within the canopy (Grant and Boehm, 2015). The 1 m in-canopy line sample measurement was positioned between 50 m and 25 m (line sample end to end) from the 5 m and 8 m single point mast measurements (Fig. 1b). The 2.8 m single point measurement was made between 45 m and 65 m from the 1-m line sample (end to end) and 18 m from the 5 and 8 m measurement mast (Fig. 1b). The N_2O in the sampled air was measured using an IRIS 4600 difference frequency generation (DFG) laser mid-infrared (IR) analyzer (ThermoFischer Scientific, Franklin, MA) with a measured N_2O minimum detection limit (MDL; 3 sigma) of 0.3 nmol mol^{-1}. The CO_2 in the sampled air was measured using a LiCOR 840 non-dispersive IR analyzer (LiCOR, Inc., Lincoln, NE) with a measured CO_2 MDL of 5 μmol mol^{-1}. The moisture content of the sampled air was also determined by the LiCOR 840 non-dispersive IR analyzer. All concentrations were corrected to dry air.

Atmospheric pressure, temperature and relative humidity were measured at 2.5 m at 5-min intervals on a weather station within 100 m of the gas measurements. Turbulence was measured at three heights (2.5 m, 5 m, and 8 m) using a 3-dimensional sonic anemometer (RM Young 81000, RM Young, Inc., Traverse City, MI). Turbulence was sampled at 16Hz and recorded at 10Hz. The minimum detection limit (MDL) was approximately 0.01 ms^{-1}. Since the tethered towers was tilted but shifted slightly in tilt due to shifts in the wind direction, a double rotation rather than planar rotation was made to correct the flow coordinate system for each 30-min turbulence-averaging interval (Lee et al, 2004). The MDL for the friction velocity (u_*), based on error propagation of the anemometer MDL through the definition of u_*, was estimated to be 0.014 ms^{-1}. In reality, the non-stationary

flow conditions in the stable nocturnal boundary layer results in sensitivity of u_* on the specific averaging period and consequently is more uncertain than the calculated MDL. Stability was assessed using the local Obukhov length (Λ) based on local measures of heat and momentum transfer within the stable boundary layer (van de Wiel et al, 2008).

The accumulation of constituent C ($Q_{accum,c}$) over the maize canopy was based on gas concentration measurements (using the DFG and NDIR instruments) made at three heights (2.8m, 5m and 8m; Fig. 1b) on an 8m tower and one height representing an integrated line concentration in the maize canopy (1 m; Fig. 1b). Accumulation flux was determined into the layer according to:

$$Q_{accum,C} = \frac{\Delta \int_0^{6.3} C dz}{\Delta t} \quad (1)$$

using Newtonian integration and assuming the concentration of C (CO_2 and N_2O) between the ground and 1 m was constant and equal to that at 1 m . The mass accumulative flux was calculated as the linear slope of the time resolved accumulation of three measurements over 90 minutes. Turbulent conditions were segregated into those with u_* less than or greater than or equal to 0.05 ms^{-1} (approximately four times the estimated sensor MDL of 0.014 ms^{-1}). This threshold was lower than that used by Pattey et al (2002), who used a threshold of 0.1 ms^{-1} for both u_* and standard deviation of w (σ_w) to estimate flux by mass accumulation and lower than that used by Wagner-Riddle et al (2007) who used a u_* threshold of 0.1 ms^{-1} and a Monin Obukhov stability of less than 2 to estimate flux by flux gradient during stable boundary conditions.

The diffusive flux of constituent C ($Q_{diff,c}$) out the top of the control volume (6.3 m^3) under both unstable and stable conditions was determined using the flux gradient method:

$$Q_{diff,C} = K_C \frac{\Delta C}{\Delta z} \quad (2)$$

where the concentration gradient ($\Delta C/\Delta z$) was calculated above the canopy between 5 m and 8 m (van de Wiel et al, 2008). The ΔC MDL was estimated at 12.7 μmol mol^{-1} for CO_2 and 0.5 nmol mol^{-1} for N_2O based on the MDL for the respective gas concentrations. The eddy exchange coefficient (K_c) for the top of the control volume was determined using 3D sonic anemometer measurements at 5m and 8m using the similarity method of Schaefer et al. (2012) and the molecular Schmidt number (0.91 for CO_2 and 0.95 for N_2O; Massman, 1998). The molecular Schmidt number was used in place of the preferred turbulent Schmidt number because no independent measure of the coefficient was possible in this experiment and literature values for the turbulent Schmidt number are quite variable (Flesch et al, 2002). Given the sonic anemometer measurement error in wind speed and the corresponding error (based on theoretical error propagation) in u_*, the error in K_c was estimated at 22%, or approximately 0.0035 m^2s^{-1}. Given the MDL of a ΔC of 18 μmol mol^{-1} CO_2, the MDL of $\Delta CO_2/\Delta z$ at 6.3 m (top of control volume) was estimated at 0.2 μmol m^{-4}. Given the MDL of a ΔC of 0.6 μmol mol^{-1} N_2O, the MDL of $\Delta N_2O/\Delta z$ at 6.3 m was estimated at 7.0 nmol m^{-4}. Diffusive fluxes where the ΔC or K_c were less than the MDL were invalidated. The MDL

of the diffusive flux (Eq. 2), based on theoretical error propagation, of CO_2 and N_2O were estimated at 0.7 nmol $m^{-2}s^{-1}$ and 0.02 nmol $m^{-2}s^{-1}$ respectively. As previously stated, the non-stationary flow conditions in the nocturnal surface boundary layer result in greater uncertainty in u_* and K_c than calculated by theoretical error propagation. In addition, since the double rotation coordinate tilt induce additional errors in u_* for u_* less than 0.15 ms^{-1} (Foken et al, 2004), the error in K_c was expected to be much lager for low turbulence conditions. Diffusive fluxes were determined over 30-min averaging time intervals. All sampling periods with invalid (below theoretical MDL) diffusive fluxes were set to zero. Z-less flow (Mahrt, 2011) was assumed to not be present at the stable control volume top: if present the method of diffusive flux calculation (Eq. 2) would be invalid.

Total nocturnal fluxes of CO_2 and N_2O over 90-minute intervals were determined by adding the 1.5 h mean of the diffusive flux (Eq. 2) to the accumulative flux (Eq. 1). Calculated fluxes were further screened for extreme outliers: values greater than ten times the standard deviation of the flux were excluded from analysis.

The CO_2 and N_2O emissions were also determined using the vented static chamber method (Mosier et al, 2006). Measurements were made between 10 h LT and 14 h LT in the 200Fa, 100Sp/100Fa and no-N treatment fields (Fig. 1). Measurements were made generally at 23 h LT in the 200Sp treatment area where the masts were located except for a four day period (5-8 August 2015) in which the diurnal variation in chamber N_2O emissions were assessed when measurements made at 00, 06, 12, and 18 h LT and measurements made at 13 h LT on 24 and 28 July. The chamber consisted of aluminium anchors (~0.74 by 0.35 by 0.12 m) driven about 0.10 m into the soil; at each sampling time lids covered the anchors to result in a chamber volume of approximately 32.4 L. On each sampling date, gas samples were collected from the chamber headspace through a rubber septum at 0, 10, 20, and 30 min after chamber deployment using a gastight syringe, and then transferred into pre-evacuated 12 mL Exetainer vials (Labco, High Wycombe, UK). Nitrous oxide and CO_2 concentrations of the gas samples were determined using a gas chromatograph (Varian 3800 GC, Mississauga, Canada) equipped with an automatic Combi-Pal injection system (Varian, Mississauga, Canada). Fluxes were calculated from the rate of change of the N_2O concentration in the chamber headspace assuming a linear rate of change in concentration within the headspace. The MDL determined based on the 99% confidence interval of the rate of change was 3.7 nmol $m^{-2}s^{-1}$ for CO_2 flux and 0.7 nmol $m^{-2}s^{-1}$ for N_2O.

Comparisons between the daily mean chamber flux and mass accumulation flux were made over three time intervals: 22 to 31 July, 1 to 22 August, and 23 August to 2 September. All valid flux measurements (chamber or accumulation) for a given day were averaged to estimate the day's flux. Only chamber measurements made in the field where the accumulation measurement were made are included. Statistics of mass accumulation measurements were made regardless of the time of day of measurement. Student's t-test was used to determine if there was a significant difference at p=0.05 between the chamber and mass accumulation measurements.

The potential influence of advection of CO_2 and N_2O from the surrounding landscape on the accumulated masses at the research site was evaluated based on 2015 land use and typical fluxes given the land use. Land use during the 2015 growing season

was assessed using CropScape Cropland Data Layer (USDA, 2017). Dominant land use, excluding developed land, was assessed for the surrounding 1 km^2 and 10 km^2 area of the measurement tower (Table 1). Fluxes associated with each land use were selected from the literature based on similarity of soil type (research site: Drummer silty clay loam), land management (research site and surrounding field tile drained, chisel plow vs. no-till with various fertilization rates and fertilizer type) and crop phenological stage (research site: maturity for soybean and maize) (Table 1). In addition, literature-reported fluxes derived using micrometeorological approaches were preferred over fluxes derived from soil chambers unless specifically reporting soil+root fluxes.

3 Results and Discussion

Measurements were made over the period 23 July to 11 September, 2015 resulting in 1685 30-min averaged records. Within this period there were 600 ½ h periods with N_2O measurements and 370 30-min periods with CO_2 measurements between 19 and 03 h LT. During this period, the mature maize canopy was 2.5 m tall (H).

3.1 Near-surface layer profiles

A common feature of the nocturnal CO_2 and N_2O concentration profiles is an increase in concentration near the surface over time (Fig. 2b,c). Mass accumulations of CO_2 and N_2O were observed over the mature maize canopy when wind speeds were low at 8 m (3.2H) (Fig. 2a). The increased concentrations were assumed to be a result of gaseous emissions largely from the soil surface. Mean wind speed (U) and the ratio of variability in w (σ_w) to u_* at both 5 m and 8 m were significantly lower when $u_* < 0.05$ ms^{-1} than when $u_* > 0.05$ ms^{-1} (Table 2; Fig. 3). Over the nocturnal period of 19 to 07 h LT, the averaged local stability at 8 m (z/Λ; van de Wiel et al, 2008) was positive regardless of u_* between 19 and 03 h LT and negative from 0300 and 0700 h LT. The negative stability expressed the influence of dawn occurring around 05 h LT (Table 2). Stable conditions (positive Λ) at 8 m occurred during 28% of the measurement periods (465 30-min measurement intervals).

Sonic temperature (T_s) increased with height between 3 and 5 m under low turbulent conditions throughout the night while increasing turbulence between 20 and 07 h LT shifted the T_s gradient from positive to negative with height (Fig. 2). However at the top of the measured profile, the temperature gradient was nearly zero for $u_* < 0.05$ ms^{-1} (Table 3). The mean bulk Richardson number (R_B) at the geometric mean height of the top two measurements averaged 2.3 when $u_* < 0.05$ ms^{-1}. For conditions with $u_* >= 0.05$ ms^{-1} the mean R_B was -1.2. Shifts in wind direction above the canopy (5 to 8 m height) were highly variable for u_* less than approximately 0.05 ms^{-1} (Fig. 3). These shifts coincided with vertical wind velocity variance less than 0.01 m^2s^{-2} and the horizontal wind velocity variance less than 0.1 m^2s^{-2} (Fig. 3). At these low turbulence conditions, turbulent transport of gases originating at the earth surface is minimal resulting in the accumulation of gases in a layer of air bounded

by a 'cap' in the surface boundary layer. The top of the surface-influenced control volume in which mass accumulation was set at 6.3 m (geometric mean of 5 m and 8 m; 2.5H) (Fig. 4).

Over the 19 to 07 h LT timeframe, the line-averaged concentrations of CO_2 at 1 m within the canopy ranged from 354 μmol mol^{-1} to 1038 μmol mol^{-1} while point concentrations at 8 m agl (5.2 m or 2.9 H above the canopy) varied from 358 μmol mol^{-1} to 862 μmol mol^{-1}. The difference between the 5 m (1.7 H) and 8 m (2.9H) CO_2 concentrations ranged from -11.4 μmol mol^{-1} to 337 μmol mol^{-1}. Eleven percent of the 90 minute mean concentration gradients at the top of the layer were high enough to calculate a turbulent diffusive flux. The mean CO_2 gradient ($\Delta CO_2/\Delta z$) was less than or equal to the MDL when $u_* > 0.05$ ms^{-1} (Table 3).

Over the19 to 07 h LT timeframe, the line-averaged N_2O concentrations within the canopy (0.4H) ranged from 0.313 μmol mol^{-1} to 0.467 μmol mol^{-1} while the point sample at 8 m ranged from 0.295 μmol mol^{-1} to 0.448 μmol mol^{-1}. The difference between the 5 m (1.7 H) and 8 m (2.9H) N_2O concentrations above the canopy ranged from -0.357 μmol mol^{-1} to 0.059 μmol mol^{-1}. Twelve percent of the 90 minute mean concentration gradients at the top of the layer were high enough to calculate a turbulent diffusive flux. The mean N_2O gradient ($\Delta N_2O/\Delta z$) was less than the MDL when $u_* > 0.05$ ms^{-1} (Table 3).

A common feature of the mean concentration profiles of both CO_2 and N_2O was a lower mean concentration from air sampled at a point 3 m (1.2H) than both the 1 m (0.4H) and 5 m (1.7H) mean concentrations. This may be a result of the close proximity of the 1.2 H point measurement to the canopy top representing only local canopy conditions. Conversely, the spatially-averaged line concentration in the canopy at 0.4H could better approximate the mean concentration at that height within the canopy. Consequently, concentration measurements at 2.8 m were excluded from all profiles prior to mass integration.

The temporal pattern of mass build-up were similar for N_2O and CO_2 (Fig. 4). The increase in either N_2O or CO_2 concentrations in the lowest 6.3 m corresponded with a decrease in wind speeds at 8 m (Fig. 2) as well as low u_* and variance in w (Fig. 4). The mean gradient in N_2O and CO_2 at this height during stable conditions and low turbulence was higher than that during higher turbulence, although the gradients varied widely (Table 3). If winds intermittently increase during the night, the concentration of both N_2O and CO_2 decreased in the surface boundary layer, with an increase occurring after the winds decline again (Figs. 1, 3). This intermittent turbulence then mixed the heat and mass further into the developing nocturnal boundary layer. The accumulation of CO_2 and N_2O in the lowest 8 m of the boundary layer might be expected to occur if the top of the layer exhibited minimal turbulence since the molecular diffusion of a gas is orders of magnitude smaller than the turbulent diffusion.

On average, the mean profiles of CO_2 and N_2O concentrations during from 19 to 03 h LT showed nearly identical concentrations at 1 m and 5 m with decrease in concentration at 8 m (Fig. 5). The corresponding mean concentration profiles for the 03 to 07 h LT time window showed no change in concentration with height (Fig. 5). Conditions during the 1900 to 03 h LT period resulted in nearly identical mean wind speed profiles regardless of u_* but substantially different temperature

profiles (Fig. 5). Temperature inversions above the canopy (2.8 m to 5 m agl) were evident between 19 and 03 h LT regardless of u_* (Fig. 5). The temperature inversion was also evident between 03 and 07 h LT when u_* was less than 0.05 ms^{-1} (Fig. 5). This near-surface inversion was not evident at the top of the accumulation control volume (between 5 m and 8 m agl) where the wind shear was high.

3.2 Mass accumulations

Using the previously-defined top of the accumulation control volume, the accumulations of N_2O and CO_2 were often evident during the night from 19 to 00 h LT with sunset approximately 21 h LT (Fig. 6). These mass accumulations corresponded with positive z/Λ (locally stable conditions) and low u_* (low turbulence). After quality assurance of the accumulated flux calculations, there were 97 90-min measurements of N_2O nocturnal flux and 78 90-min measurements of CO_2 nocturnal flux with u_* less than 0.05 ms^{-1}. Note that the mean gradients of both N_2O and CO_2 were less for this set of measurements (Table 4) than for all measurement periods (Table 3).

Accumulated N_2O flux during low turbulence and no measureable diffusive flux across the control volume top averaged 0.22 nmol $m^{-2}s^{-1}$ with a variability (standard deviation) greater than the mean (Table 4). The accumulated fluxes of N_2O between 19 h LT and 03 h LT were relatively steady over the measurement period (Fig. 8). Accumulations within the control volume were greater (0.58 nmol $m^{-2}s^{-1}$) during the 22% of the measured flux periods when there was measureable diffusive flux out the top of the control volume (Table 4). When measureable, the diffusive flux of N_2O was twice the accumulative flux (Table 4) resulting in a mean total measured N_2O flux (accumulative + diffusive) of 0.53 nmol $m^{-2}s^{-1}$ (SD=0.25 nmol $m^{-2}s^{-1}$). This suggests that the ability to estimate diffusion across the upper boundary was limited by the N_2O gradient. These fluxes were similar to median daily flux gradient-derived fluxes for maize grown over two years in a similar climate (Ontario, Canada) on imperfectly drained silt-loam soils with conventional tillage (0.5 nmol $m^{-2}s^{-1}$) but lower than that for no-till (Wagner-Riddle et al, 2007, Table 1).

The accumulated CO_2 fluxes between 19 h LT and 03 h LT generally decreased over time with values ranging from approximately 2.0 to 0.2 μmol $m^{-2}s^{-1}$ (Fig. 7). The mass accumulative flux during low turbulence averaged 0.40 μmol $m^{-2}s^{-1}$ with a variability less than the mean (Table 4). Measurable diffusive CO_2 flux out of the control volume, occurring 23% of the low turbulence CO_2 flux events, corresponded with only slightly lower accumulative fluxes (0.37 μmol $m^{-2}s^{-1}$; Table 4). This suggested that the limiting factor in estimating diffusion across the control volume was the turbulent exchange process not the concentration gradient. When measureable, the diffusive flux of was nine times the accumulative flux (Table 4), resulting in a mean total measured CO_2 flux (accumulative + diffusive) of 1.16 μmol $m^{-2}s^{-1}$. (SD=0.49 μmol $m^{-2}s^{-1}$). This flux was substantially lower than eddy-covariance-derived nocturnal mean flux over maize fields (10.8 to 30.0 μmol $m^{-2}s^{-1}$) in a similar climate (Ontario, Canada) during the same period in the growing season but under more turbulent winds: mean wind speeds of at least 1.5 ms^{-1} and u* between 0.075 and 0.1 ms^{-1} (Pattey et al, 2002) compared to mean wind speeds of 1.1 ms^{-1} and u* of 0.02 ms^{-1}.

Greater turbulence (higher u_* at 8 m) did not affect the accumulative N_2O flux in the control volume if no diffusion was measurable but did reduce the flux when there was measureable diffusion (Table 4). Greater turbulence reduced the accumulative CO_2 flux whether or not there was measureable diffusion (Table 4). The greater turbulence corresponded with a decrease in the mean N_2O gradient and an increase in the CO_2 gradient at the top of the control volume and increased diffusive flux out of the control volume (Table 4). The upper transport 'cap' to the mass accumulation control volume was on average stronger for the low turbulence condition than the higher turbulence condition (based on σ_w and σ_w/u_*; Table 2) and the eddy diffusivities were lower (Table 3). The effectiveness of this 'cap', separating the developing nocturnal boundary layer above from the surface boundary layer below, had a larger effect on the mass accumulation of CO_2 than N_2O and a greater effect on the diffusive flux of N_2O than CO_2 (Table 4). This might be expected if the local CO_2 flux was more similar to the more distant surroundings (more homogeneous) than the N_2O flux. It is important however to note that the high variability in CO_2 and N_2O fluxes under low turbulence resulted in mean accumulative fluxes with or without measureable diffusive flux that was not statistically different (Student t-test; p=0.05) (Table 4).

Eddy diffusivities were comparable to and exhibited the same relationship to u_* and z/Λ for positive z/Λ as those reported for N_2O and NH_3 in Schaefer et al. (2012). The mean eddy diffusivities were more than an order of magnitude higher for conditions with $u_* > 0.05$ ms^{-1} than $u_* < 0.05$ ms^{-1} (Table 3). Clearly the u_* threshold of 0.05 ms^{-1} still allowed for weak turbulent diffusion of both N_2O and CO_2 out of the near-surface control volume and into the nocturnal boundary layer in 22% and 23% (respectively) of the flux events (Table 4). The general relatively high diffusive versus accumulative flux (Table 4) during low turbulence conditions however may also be a result of a combination of non-stationarity of the flow and/or anemometer tilt. Assuming stationary flow and no anemometer tilt, the approximation of the eddy diffusivities of N_2O and CO_2 by substituting molecular Schmidt numbers for turbulent Schmidt numbers likely contributed to underestimated flux values since these Schmidt numbers were higher than the generalized turbulent Schmidt number of Flesch et al (2002).

3.3 Soil chamber fluxes

The soil chamber CO_2 and N_2O flux measurements, made at various hours of the day during the measurement period, also showed a decreasing flux over the period (Figs. 7, 8). CO_2 flux in the 200Sp treatment, where the profile measurements were made, ranged from 0.1 μmol m^{-2}s^{-1} to 2.1 μmol m^{-2}s^{-1} and averaged 0.9 μmol m^{-2}s^{-1}. These chamber measurements had a mean signal to noise ratio of 250. These fluxes are similar to soil+root respiration fluxes reported in the literature for maize fields (Table 1). The region of the south field in which no N was applied during the past year (Fig. 1) had a mean CO_2 emission of 0.5 μmol m^{-2}s^{-1}, averaging 50% of the mean field emissions under various N treatments and similar to that reported for soil+root respiration of soybean in the literature (Table 1). Although most measurements were made at 23 h LT, some of the variability in chamber measurements was a result of the time of measurement. The four-day study of diurnal variation in mean hourly CO_2 emissions ranged from 1.04 μmol m^{-2}s^{-1} to 1.48 μmol m^{-2}s^{-1} with the highest emissions at 18 h LT with a ratio of midnight to noon LT emissions of 1.2.

Nitrous oxide fluxes in the 200Sp treatment field ranged from 0.3 nmol $m^{-2}s^{-1}$ to 2.2 nmol $m^{-2}s^{-1}$ averaging 1.1 nmol $m^{-2}s^{-1}$. These fluxes were lower than commonly reported in the literature for maize but similar to that of soybeans (Table 1). This may be due to the negligible amount of the applied nitrogen available for denitrification and nitrification in the maize field. These chamber N_2O measurements thus had a mean signal to noise ratio of 1.7. The fields on which no N was applied during the year had a mean emission of 0.59 nmol $m^{-2}s^{-1}$; 54% of the mean fertilized field emissions and equal to the Chamber method MDL. As with the CO_2 flux measurements, some of the variability in chamber measurements was a result of the time of measurement. The four-day study of diurnal variation in mean hourly N_2O emissions ranged from 0.96 nmol $m^{-2}s^{-1}$ to 1.40 nmol $m^{-2}s^{-1}$ with the highest emissions at 18 h LT with a ratio of midnight to noon LT emissions of 0.93.

3.4 Comparative fluxes

As with the comparison of CO_2 fluxes determined by eddy covariance and boundary-layer mass balance (Eugster and Siegrist, 2000), the fluxes determined by chamber and mass accumulation are local and 'regional' fluxes respectively. The CO_2 flux measurements based on mass accumulation within the control volume but not diffusion across the control volume top were generally lower than the chamber measurements with the exception of a few outlier high mass accumulation values (Fig. 7). Inclusion of measureable diffusive flux to the accumulative flux resulted in total flux estimates more similar to soil chamber measurements. Average mean daily CO_2 flux estimates for two of the three measurement time periods indicated the total mass accumulation method flux was between 0.9 and 1.3 of that determined by the chamber method (Table 5). Higher accumulation flux over the chamber flux was expected due to the chamber flux method measured only root and soil respiration while the mass accumulation flux method measured the respiration of the soil, roots, stalks and leaves. This can result in a large difference in flux: Parkin et al (2005) measured soil and root respiration with chambers and whole canopy respiration by eddy covariance and found that the soil respiration was approximately 50% of the total measured CO_2 flux. Given the variability in daily flux estimates within each period, the fluxes determined by chamber and mass accumulation methods were not significantly different (Table 5).

The N_2O flux measurements based on mass accumulation under low turbulence and stable conditions were generally much lower than those measured using the chambers on the same day (Fig. 8). Inclusion of measureable diffusive fluxes in the flux estimates over three measurement time periods showed that the accumulation method estimated mean daily fluxes only 60% to 80% of the soil chambers (Table 5). Again, given the variability in mean daily flux estimates within each time period, the fluxes determined by the chamber and mass accumulation methods were not significantly different (Table 5).

Differences between the accumulation flux versus chamber flux measurements were likely in part due to the advection of gas emitted from surrounding fields. The accumulated mass of CO_2 and N_2O have contributions from local soils sources as well as mass advection from more distant sources due to the meandering nature of the air flow during the stable nocturnal conditions (Eugister and Siegrist, 2000). Unfortunately, the analytical approaches to defining the flux footprint do not apply to the stable nocturnal conditions in which the accumulations occur ($z/\Lambda > +1$, $u_* < 0.05$ ms^{-1}; Vesala et al, 2007), although they are believed

to be in the order of ten kilometers (eg. Chambers et al, 2011). At scales of kilometres (10 km^2 area), the land use was crop agriculture; dominated by nearly equal soybean and maize production (46% and 47% respectively with an addition 2% in grass in the (Table 1). Within the nearest square kilometre around the research site, maize production dominated the land use (Table 1).

The CO_2 flux of the un-fertilized fields were similar to those of the fertilized fields (Fig. 7). The measured fluxes were substantially lower than those for other maize fields as well as grass and soybean fields reported in the literature (Table 1). If anything, it is reasonable to assume that the advected, regionally-emitted CO_2 from surrounding soybean and maize production would have increased the accumulation flux estimates. However the relatively low accumulation fluxes suggest that advection did not substantially contribute to the measured mass accumulation. The measured chamber N_2O flux from un-fertilized fields of maize was typically lower than fertilized maize fields and closer to the flux measured by the accumulation method (Fig. 8). Since roughly one-half the surrounding area was in soybean production (Table 1), it is reasonable to assume horizontal advection of air with higher N_2O concentration from nearby grass and soybean canopies could have potentially affected the N_2O profile. However, literature values for fluxes from surrounding grassy areas and soybean fields (Table 1) are generally similar to the flux measured by the accumulation method in a fertilized maize field (Table 5). Consequently there is little evidence to support the supposition that advection contributed significantly to the accumulated mass.

The general underestimate of CO_2 and N_2O fluxes using the mass accumulation method may also be a result of using two small of an accumulation volume. The 'cap' of the volume was arbitrarily set at the geometric mean between the upper two measurement heights. An objective measure of the 'cap' height is needed. Given the significantly greater flux associated with diffusion out the top of the accumulation control volume relative to the computed accumulated flux within the control volume (Table 4), the accumulation control volume was likely too shallow.

4 Conclusions

Nocturnal CO_2 and N_2O emissions from the soil surface were determined by measuring the accumulation of mass within a mixing-limited surface boundary layer control volume and the diffusion of mass out the top of the control volume. The magnitude of the accumulations influenced the ability for the accumulation method to be effective at estimating nocturnal flux: CO_2 flux determined by the accumulation method were comparable to those measured using the chamber method while that for N_2O were below that measured using the chamber method. For the N_2O flux, there is no known canopy flux of N_2O and consequently the chamber method and accumulation method should have been comparable. Measurement errors associated with a limited vertical dimension to the control volume, non-stationarity of low turbulent flow in the stable nocturnal surface boundary layer, and estimating the Schmidt number for the diffusive flux component likely contributed to the differences between the accumulation and chamber flux methods. Advection during the stable nocturnal conditions did not appear to contribute to the measured profiles and the subsequent estimate of N_2O flux or CO_2 flux. Additional work is needed to evaluate the use of the accumulation method for N_2O fluxes for accumulations within a larger vertical domain to the control volume

and more homogeneous regional land use in conjunction with using chamber methods with a lower MDL (higher signal to noise ratio).

Author Contribution

R. Grant designed, conducted and analysed the mass accumulation experiment while R. Omonode conducted the chamber gas flux measurements. R. Grant prepared the manuscript with contributions from R. Omonode.

Competing interests

The authors declare that they have no conflict of interest.

Acknowledgements

The authors appreciate the field technical assistance of Cheng Hsien Lin and Austin Pearson.

References

Acevedo, O.C., Moraes, O.L., DaSilva, R., Fitzjarrald, D.R., Sakai, R.K., Staebler, R.M. and Czikowsky, M.J.: Inferring nocturnal surface fluxes from vertical profiles of scalers in an Amazon pasture. Global Change Biology 10, 886-894, 2004.

Acevedo, O.C., DaSilva, R., Fitzjarrald, D.R., Moraes, O.L., Sakai, R.K. and Czikowsky, M.J.: Nocturnal vertical CO2 accumulation in two Amazonian ecosystems. J. Geophy. Res. 113, G00b004, doi:10.1029/2007JG000612, 2008.

Aubinet, M., Feigenwinter, C., Heinesch, B., Laffineur, Q., Papale, D., Reichstein, M., Rinne, J. and van Gorsel, E.: Chapter 5: Nightime flux correction, In: Aubinet, M., Vesala, T. and Paple, D. (eds) Eddy Covariance: A Practical Guide to Measurements and Data Analysis. Springer Atmospheric Sciences, doi 10.1007/978-94-007-2351-1_5, pp 133-172, 2012.

Biraud, S., Ciais, P., Ramonet, M., Simmonds, V.K., Monfrey, P, O'Doherty, S, Spain, G, Jennings, S.G.: Quantification of carbon dioxide, methane, nitrous oxide and chloroform emissions over Ireland from atmospheric observations at Mace Head. Tellus 54B, 41-60, 2002.

Bowden, R.D., Rullo, G., Stevens, G.R. and Steudler, P.A.: Soil fluxes of carbon dioxide, nitrous oxide and methane at a productive temperate deciduous forest. J. Environ. Qual. 29, 268-276, 2000.

Bremner, J.M., Breitenbeck, G.A. and Blackmer, A.M.: Effect of anhydrous ammonia fertilization on emission of nitrous oxide from soils. J. Environ. Qual.10, 77-80, 1981.

Bremner, J.M., Robbins, S.G. and Blackmer, A.M.: Seasonal variability in emissions of nitrous oxide from soil. Geophys. Res. Lett. 7, 641-644, 1980.

Chamber, S., Williams, A.G., Zahorowski, W., Griffiths, A. and Crawford, J.: Separating remote fetch a local mixing influences on vertical radon measurements in the lower atmosphere. Tellus 63B, 843-859, 2011.

De Costa, J.M.N., Rosenberg, N.J., and Verma, S.B.: Respiratory release of CO2 in alfalfa and soybean under field conditions. Agric. Forest Meteorol. 37, 143-158, 1986.

De Jong, E., Schappert, H.J.V. and McDonald, K.B.: Carbon dioxide evolution from virgin and cultivated soil as affected by management practices and climate. Ca. J. Soil Sci. 54, 299-307, 1974.

Draxler, R.R. and Hess, G.D.: An overview of the HYSPLITY-4 modelling system for trajectories, dispersion, and deposition. Aust. Meteorol. Mag. 47, 295-308, 1998.

Duxbury, J.M. and Bouldin, D.R.: Emissions of nitrous oxide from soils. Nature (London) 298, 462-262, 1982.

Eichner, M.J.: Nitrous oxide emissions from fertilized soils: summary of available data. J. Environ. Qual. 19, 272-280, 1990.

Eugster, W. and Siegrist, F.: The influence of nocturnal CO_2 advection on CO_2 flux measurements. Basic Appl. Ecol. 1,177-188, 2000.

Flesch, T.K., Prueger, J.H., Hatfield, J.L.: Turbulent Schmidt number from a tracer experiment. Agric. Forest Meteorol. 111, 299-307, 2002.

Foken, T., Goeckede, M., Mauder, M., Mahrt, L., Amiro, B. and Munger, W.: Post field data quality control. In: Lee, X., Massman, W., Law, B. (Eds). Handbook of Micrometeorology, Kluwer Academic Pub, Dordrecht, Netherlands. pp. 181-208, 2004.

Grant, R.H. and Boehm, M.T.: Manure ammonia and hydrogen sulfide emissions from a western dairy storage basin. J. Environ. Qual. 44, 1-10, 2015.

Hendrix, P.F., Han, C.- R. and Groffman, P.M.: Soil respiration in conventional and no-tillage ecosystems under different winter cover crops. Soil Tillage Res. 12, 135-158, 1988.

Kaimal, J.C. and Finnigan, J.J.: Atmospheric Boundary Layer Flows: their structure and measurement. Oxford Univ. Press, NY, NY 289p, 1994.

Lee, X., Black, T.A., den Hartog, G, Neumann, H.H., Nesic, Z. and Olejnik, J.: Carbon dioxide exchange and nocturnal processes over a mixed deciduous forest. Agric. Forest Meteorol. 81, 13-29, 1996.

Lee, X., Finnigan, J. and Paw U, K.T.: Coordinate systems and flux bias error. In: Lee, X., Massman, W., Law, B. (Eds). Handbook of Micrometeorology, Kluwer Academic Pub, Dordrecht, Netherlands. pp 33-66, 2004.

Mahrt, L.: The near-calm stable boundary layer. Boundary Layer Meteorol. 140, 343-360, 2011.

Massman, W.J.: A review of the molecular diffusivities of H_2O, CO_2, CH_4, CO, O_3, SO_2, NH_3, N_2O, NO, and NO_2 in air, O_2 and N_2 near STP, Atmos. Environ. 32, 6, 111-1127, 1998.

Mosier, A, Shimel, D., Valentine, D., Bronson, K. and Parton, W.: Methane and nitrous oxide fluxes in native, fertilized and cultivated grasslands. Nature 350, 330-332, 1991.

Omonode, R.A., Vyn, T.J., Smith, D.R., Hegymegi, P., Gal, A.: Soil carbon dioxide and methane fluxes from long-term tillage systems in continuous corn and corn-soybean rotations. Soil Tillage Res. 92, 182-195, 2007.

Parkin, T.B. and Kaspar, T.C.: Nitrous oxide emissions from corn-soybean systems in the Midwest. J. Environ. Qual. 35, 1496-1506, 2006.

Parkin, T.B., Kaspar, T.C., Sennwo, Z., Prueger, J.H. and Hatfield, J.L.: Relationship of soil respiration to crop and landscape in the Walnut Creek watershed. J. Hydromet. 6, 812-824, 2005.

Pattey, E, Strachan, I.B., Desjardins, R.L. and Massheder, J.: Measuring CO_2 flux over terrestrial ecosystems using eddy covariance and nocturnal boundary layer methods. Agric. Forest Meteorol. 113, 145-158, 2002.

Pendall, E., Schwendenmann, L., Rahn, T., Millers, J.B. and Tans, P.P.: Land use and season affect fluxes of CO_2, CH_4, CO, N_2O, H_2 and isotopic source signatures in Panama: evidence from nocturnal boundary layer profiles. Global Change Biol. 16, 2721-2736, 2010.

Raich, J.W. and Tufekcioglu, A.: Vegetation and soil respiration: correlations and controls. Biogeochem. 48, 71-90, 2000.

Schaefer, K., Grant, R.H., Emeis, S., Raabe, A., von der Heide, C. and Schmid, H.P.: Areal-averaged trace gas emission rates from long-range open-path measurements in stable boundary layer. Atmos. Meas. Tech. 5, 1571-1583, 2012.

Tufekcioglu, A., Raich, J.W., Isenhart, T.M., Schultz, R.C.: Soil respiration within riparian buffers and adjacent fields. Plant Soil 229, 117-124, 2001.

USDA: Cropscape- Cropland Data Layer. Center for Spatial Information Science and Systems, National Agricultural Statistics Service, United States Department of Agriculture, https://nassgeodata.gmu.edu/CropScape/, (accessed 6/15/2017)

van de Wiel, B.J.H., Moene, A.F., De Ronde, W.H. and Jonker, H.J.J.: Local similarity in a stable boundary layer and mixing-length approaches: consistency of concepts. Boundary-Layer Meteorol. 128, 103-116, 2008.

Vesala, T., Kljun, N., Rannik, Ü., Rinne, J., Sogachev, A., Markkan, T., Sabelfeld, K., Foken, Th. and Lecelerc, M.Y.: Flux and concentration footprint modelling**:** State of the art. Envon. Poll. 152, 653-666, doi:10.1016/**j**.envpol.2007.06.070, 2007.

Venterea, R.T., Burger, M. and Spokas, K.A.: Nitrogen oxide and methane emissions under varying tillage and fertilizer management. J. Environ Qual. 34, 1467-1477, 2005.

Wagner-Riddle, C., Furon, A., McLaughlin, N.L., Lee, I., Barbeau, J., Jayasundrara, S., Parkin, G. and von Bertold, P.: Intensive measurement of nitrous oxide emissions from a corn-soybean-wheat rotation under two contrasting management systems over 5 years. Global Change Biol. 13, 1722-1736, 2007.

Xia, Y., Conen, F., Haszpra, L., Ferenczi, Z. and Zahorowski, W.: Evidence for nearly complete decoupling of very stable nocturnal boundary layer overland. Boundary-Layer Meteorol. 138, 163-170, 2011.

Table 1: 2015 Land use around the research site and literature-reported CO_2 and N_2O fluxes for each land use.

Land use	1 km^2 area (%)[1]	10 km^2 area (%)[1]	CO_2 respiration ($\mu mol\ m^{-2}\ s^{-1}$)	Source	N_2O emissions (nmol $N_2O\ m^{-2}\ s^{-1}$)	Source
Maize production	83	47	Soil/root: 0.9-1.8 Canopy:11.7-15.8	Omonode et al, 2007 Pattey et al, 2002	0- 2.1 0.5-2.3 0.2-0.5	Eichner, 1990 Parkin and Kaspar, 2006 Wagner-Riddle et al, 2007
Soybean production	15	46	Soil/root: 2.9 Canopy: 3.6,4.3 Soil/root: 0.41,0.49 Canopy: 3.8 Canopy:17.5	Raich & Tufekcoglu, 1999; DeCosta, et al, 1986 Parkin et al, 2005 Pattey et al, 2002	0.3-1.2 1.7-2.0	Bemner et al, 1980 Parkin and Kaspar, 2006
Grass	2	2	Canopy: 3.5	Tufekcoglu,et al 2001	0.2 0.3	Eichner, 1990 Mosier et al, 1991
Deciduous Forest	0	1	Soil/root: 2.2,2.5 Canopy: 5.2	Raich &Tufekcoglu, 1999 Lee at al, 1996	<0.3-0.6, 1.2	Bowden et al, 2000; Goodroad & Keeney, 1984
Bare ground	0	<1	Soil: 0.06,0.06,0.06	DeCosta, et al, 1986	1.4-2.0 (fertilized)	Bremner et al, 1981
Alfalfa	0	<1	Canopy: 1.7 Soil/root: 1.1	DeCosta, et al, 1986	1.7-4.3	Duxbury and Bouldin, 1982

1: Land use during the 2015 growing season assessed using CropScape Cropland Data Layer (USDA,2017).

Table 2: Wind conditions over the maize canopy. Statistics based on 30-min averaging period of 10Hz 3D sonic anemometer measurements at indicated heights over the entire study period.

			8 m		5 m			8 m		
Time interval (LT)	**Flow condition at 8 m**	**Statistic**	**$U^{\dagger}$ (ms^{-1})**	**$z/\Lambda^{\ddagger}$**	**Friction velocity-u_* (ms^{-1})**	**Standard deviation of vertical velocity–σ_w (ms^{-1})**	**σ_w/u_***	**Friction velocity-u_* (ms^{-1})**	**Standard deviation of vertical velocity–σ_w (ms^{-1})**	**σ_w/u_***
1900-0300	Low turbulence u_*<=0.05 ms^{-1} n^{+}=290	Mean	1.05	16.05	0.04	0.003	0.066	0.02	0.002	0.080
		Standard deviation	0.45	0.80	0.02	0.003	0.152	0.01	0.002	0.176
	Turbulent u_*>0.05 ms^{-1} n=314	Mean	2.17	0.10	0.21	0.089	0.421	0.19	0.083	0.435
		Standard deviation	0.94	0.04	0.14	0.067	0.488	0.13	0.104	0.800
0300-0700	Low turbulence u_*<=0.05 ms^{-1} n=157	Mean	0.98	-3.43	0.04	0.003	0.072	0.03	0.002	0.086
		Standard deviation	0.44	0.32	0.02	0.004	0.204	0.01	0.004	0.322
	Turbulent u_*>0.05 ms^{-1} n=923	Mean	2.80	-1.33	0.36	0.212	0.593	0.33	0.200	0.605
		Standard deviation	1.45	0.00	0.17	0.188	1.090	0.17	0.171	1.021

†: U=wind speed

‡: Λ= Local Obukhov length

+: n= number of 30-min measurements

Table 3: Characteristics of the nocturnal boundary layer at the top of the accumulation control volume with stable conditions (positive local Obukhov length) at 8m. Statistics based on 30-min averaging periods.

Time interval (LT)	Flow condition at 8 m agl	6.3 m agl					
		Statistic	$\Delta T_s^{\dagger}/\Delta z$ ($^oC\ m^{-1}$)	$\Delta N_2O/\Delta z$ ($\mu mol\ m^{-4}$)	$\Delta CO_2/\Delta z$ ($mmol\ m^{-4}$)	$K^{\ddagger}_{N2O}$ ($m^2\ s^{-1}$)	K_{CO2} ($m^2\ s^{-1}$)
1900-0300	Low turbulence u_*^{+}<=0.05 ms^{-1}	Mean	-0.008	0.08	1.11	0.008	0.008
		Standard deviation	0.033	0.14	1.23	0.024	0.022
	Turbulent u_*>0.05 ms^{-1}	Mean	0.148	0.00	0.21	0.233	0.221
		Standard deviation	0.025	0.09	0.38	0.229	0.216
0300-0700	Low turbulence u_*<=0.05 ms^{-1}	Mean	0.005	0.06	0.82	0.010	0.009
		Standard deviation	0.053	0.09	0.96	0.111	0.105
	Turbulent u_*>0.05 ms^{-1}	Mean	0.270	0.00	0.02	0.601	0.568
		Standard deviation	0.035	0.19	0.18	0.307	0.290

+: u_* =friction velocity

†: T_s =sonic temperature

‡: K =diffusion coefficient

n

Table 4: Flux of N_2O and CO_2 across the top of the accumulation control volume during stable (positive local Obukhov length) nocturnal conditions between 19 and 07 h LT. Accumulation flux based on 90-min mass accumulations. Diffusive flux based on average of three ½ hour gradients.

Flow condition at 8 m	Statistic	Gradient at top of control volume (6.3 m agl)		N_2O accumulation flux (nmol $m^{-2}s^{-1}$)		N_2O diffusive flux (nmol $m^{-2}s^{-1}$)	CO_2 accumulation flux (μmol $m^{-2}s^{-1}$)		CO_2 diffusive flux (μmol $m^{-2}s^{-1}$)
		N_2O (μmol m^{-4})	CO_2 (mmol m^{-4})	without measurable diffusion	with measurable diffusion		without measurable diffusion	with measurable diffusion	
Low turbulence u_*^+<=0.05 ms^{-1}	Mean	0.04	0.43	0.22	0.58	1.06	0.40	0.37	3.33
	SD‡	0.06	0.48	0.17	0.62	1.37	0.29	0.32	3.58
	n†	89	67	76	21	21	60	18	18
Turbulent u_*>0.05 ms^{-1}	Mean	0.02	0.64	0.19	0.49	3.23	0.11	0.13	5.87
	SD	0.04	0.64	0.18	0.82	1.92	0.11	0.11	2.48
	n	59	59	58	5	5	65	26	26

+: u_*=friction velocity

‡: SD=standard deviation

†: n= number of 90-min values

Table 5: Comparative mean daily fluxes of N_2O and CO_2 across three similar flux periods.

	Total mass accumulation flux (including accumulative and diffusive flux when measureable)			Chamber flux in Sp200 treatment field			Ratio
Measurement period (DD/MM/YY)	n*	Mean	Standard deviation	n*	Mean	Standard deviation	Mass accumulation/ Chamber
CO_2	(#)	(μmol $m^{-2}s^{-1}$)	(μmol $m^{-2}s^{-1}$)	(#)	(μmol $m^{-2}s^{-1}$)	(μmol $m^{-2}s^{-1}$)	
22/07/15-31/07/15	-	-	-	2	1.60	0.37	-
01/08/15-22/08/15	12	0.76	0.60	11	0.83	0.44	0.9
23/08/14-2/09/15	4	0.21	0.08	2	0.16	0.10	1.3
N_2O	(#)	(nmol $m^{-2}s^{-1}$)	(nmol $m^{-2}s^{-1}$)	(#)	(nmol $m^{-2}s^{-1}$)	(nmol $m^{-2}s^{-1}$)	
23/07/15-31/07/15	5	1.20	0.83	2	1.93	0.34	0.6
01/08/15-22/08/15	14	0.76	0.18	11	1.00	0.35	0.8
23/08/14-10/09/15	7	0.25	0.15	2	0.40	0.22	0.6

*= number of days with valid measurements

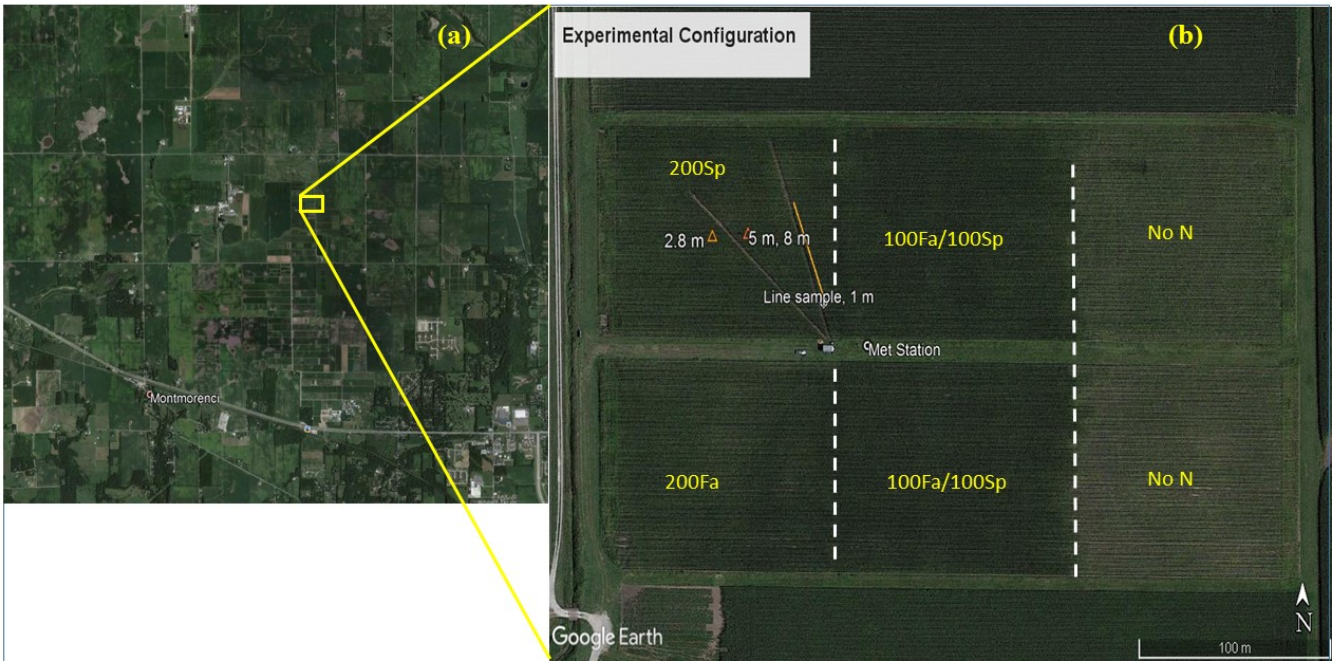

Figure 1: Experimental domain: GoogleEarth® images from August 2015 showing the homogeneous agricultural land use across the region surrounding the experimental field (Montmorenci, Indiana, USA; 40.495º latitude and -86.994º longitude: panel a) and the configuration of measurements in the experimental field (panel b). Fertilizer treatments (kgN Ha^{-1}/Season) in the north field and south field (200Sp, 200Fa, 100Sp/100Fa, and No N) as well as the locations and heights of the sonic anemometers and inlets (open triangles), integrated line sample (open diamond and orange line), and meteorological station (open circle) are indicated in panel b. Note scale in lower right corner of panel b.

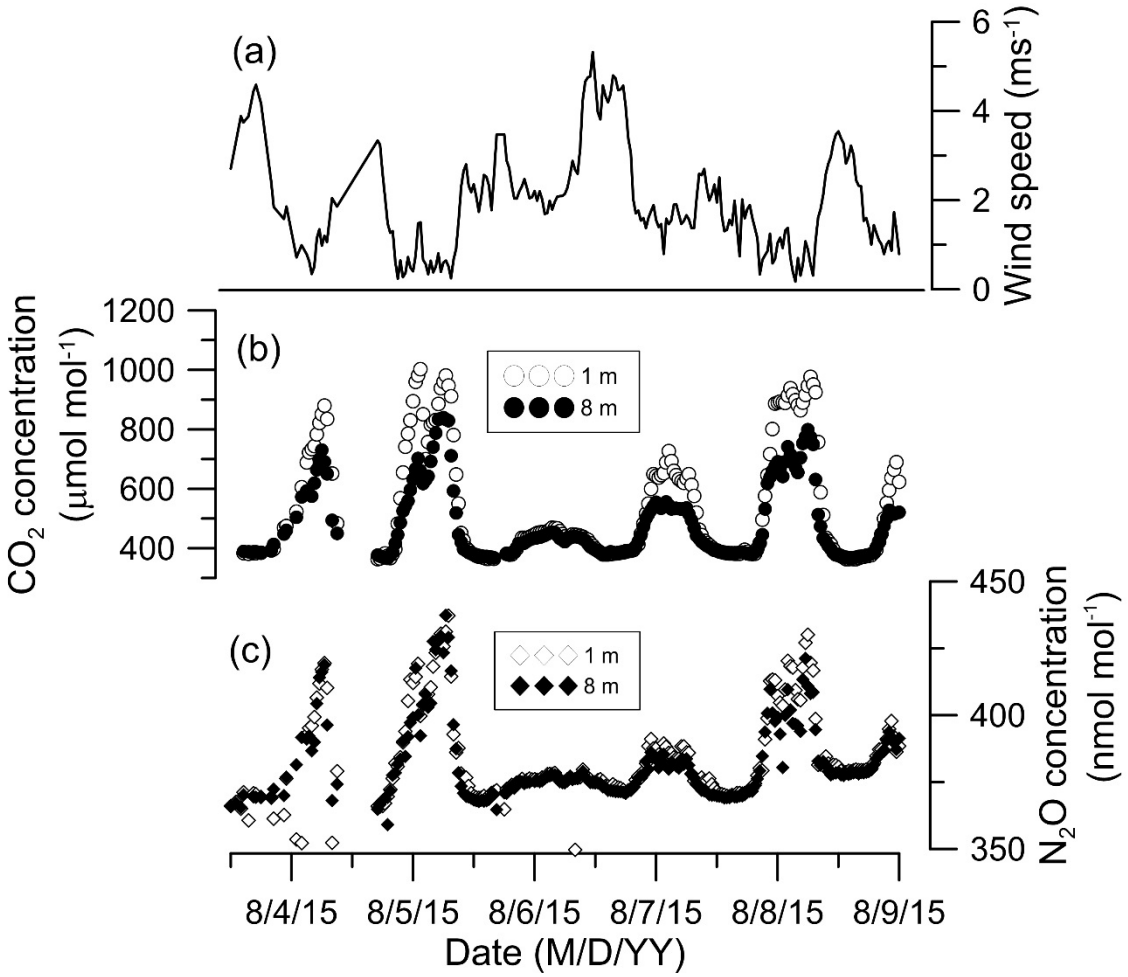

Figure 2: Changes in CO_2 and N_2O concentrations at the bottom and top of the measured control volume relative to wind speed at 8 m. The wind speed at 8m (panel a, right ordinate), the CO_2 concentrations at 1 m and 8 m (panel b, left ordinate) and the N_2O concentrations at 1 m and 8 m (panel c, right ordinate) are indicated for a five-day period. Dates on the abscissa are indicated at the beginning of the indicated day (midnight). Note the increase in wind speed during the 8/5/15 night corresponds with a decrease in both the 1 m and 8 m concentrations of both CO_2 and N_2O. Date/time is local time.

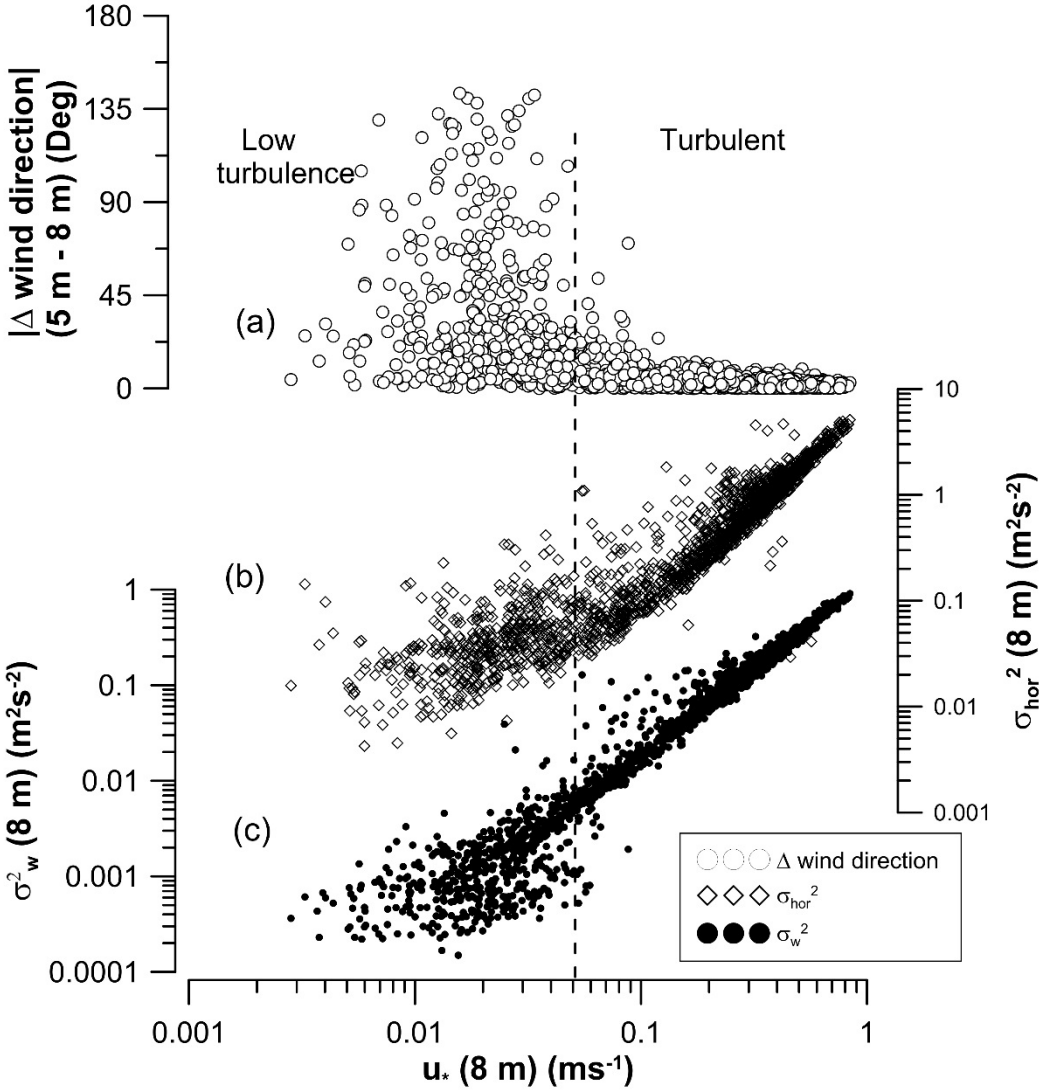

Figure 3: Wind conditions in the near-surface layer over the entire study period. The relationship between absolute value of change in wind direction (panel a with ordinate axis to left), horizontal wind velocity variance (σ_{hor}^2; panel b with ordinate axis to left) and the vertical wind velocity variance (σ_w^2; panel c with ordinate axis to right) with friction velocity (u_*) is indicated. The dashed line demarcates the separation of 'low turbulence' and 'turbulent' classifications for wind conditions. Note that the demarcation between 'low turbulence' and 'turbulent' flow corresponds with a σ_w^2 threshold of 0.01 m^2s^{-2}.

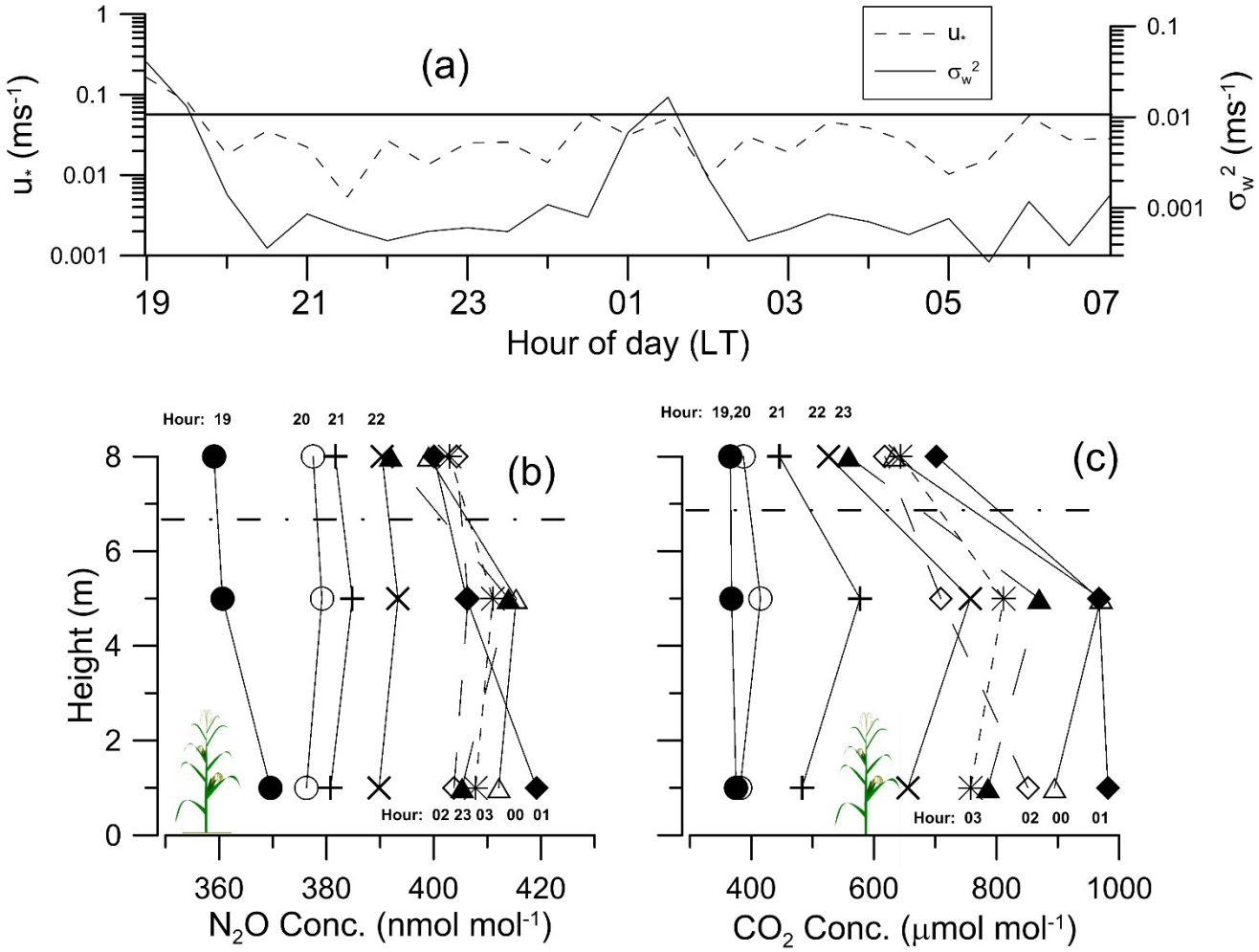

Figure 4: Near-surface atmospheric conditions during the night of 5 August, 2015. The friction velocity (u_*, left ordinate) and vertical wind velocity variance (σ_w^2, right ordinate) at 8 m are indicated from 19 to 07 h LT in panel a. The solid line (panel a) indicates the upper thresholds for the 'low turbulence' classification. Labelled profiles (h LT) of N_2O and CO_2 concentrations every hour from 19 h LT until 03 h LT are indicated with differing symbols and lines in panels b and c. Note the 01-02 h LT burst of vertical wind variance (panel a) corresponds with losses in N_2O (panel b) and CO_2 (panel c). Sunrise and sunset times were approximately 07 h and 21 h LT.

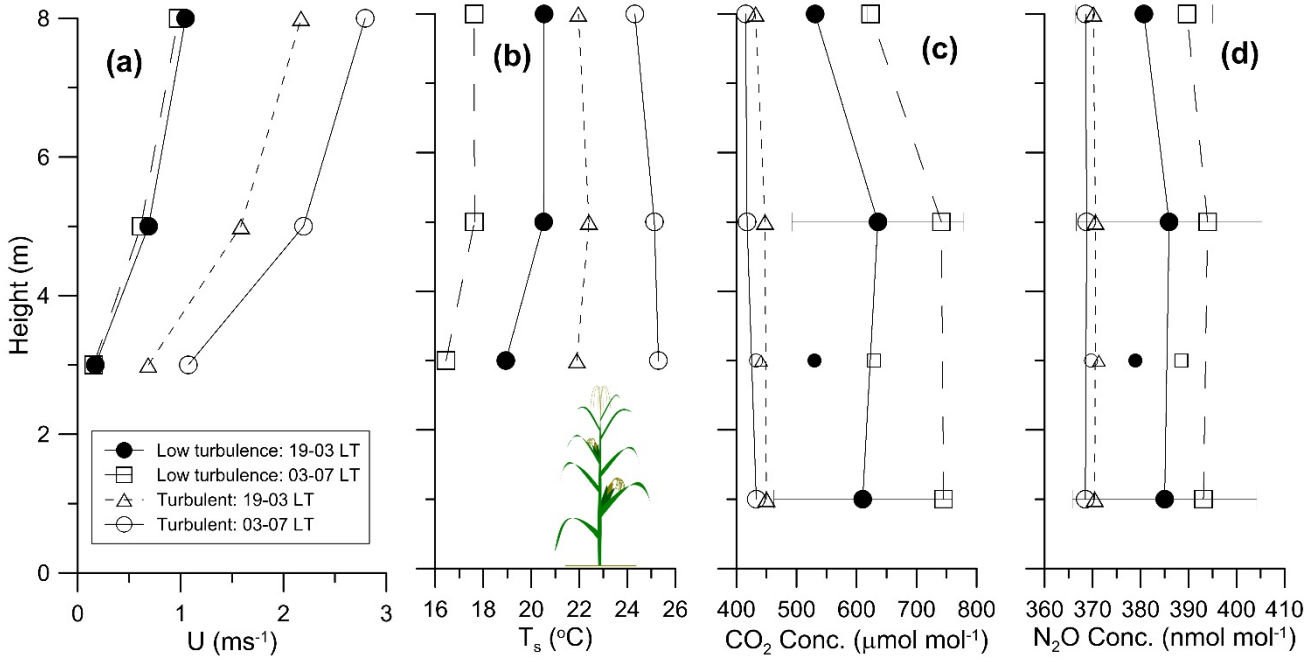

Figure 5: Mean profiles of wind speed, sonic temperature, and concentrations of CO_2 and N_2O under different friction velocity and time domain classes for the entire study period. The mean wind speed (U, panel a), sonic temperature (T_s; panel b), and concentration profiles of CO_2 (panel c) and N_2O (panel d) when the air at 8 m had low turbulence ($u_* < 0.05$ ms^{-1}) or turbulent ($u_* >= 0.05$ ms^{-1}) between 19 and 03 h LT and 03 and 07 h LT are indicated. Canopy height was 2.8 m. Smaller symbols not connected with lines represent concentration measurements excluded from mass accumulations due to their close proximity to the canopy top.

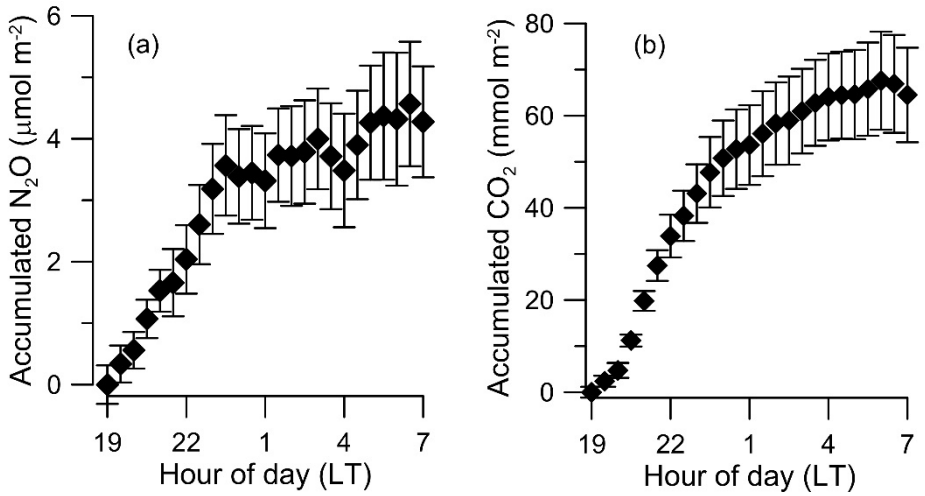

Figure 6: Accumulation of CO_2 and N_2O within the lowest 6.3m of the boundary layer during the night throughout the study period. The mean accumulations of N_2O (panel a) and CO_2 (panel b) are indicated with vertical error bars indicating the standard error of the mean of each 30-min mean accumulation. Sunrise was approximately 06 to 07 h LT.

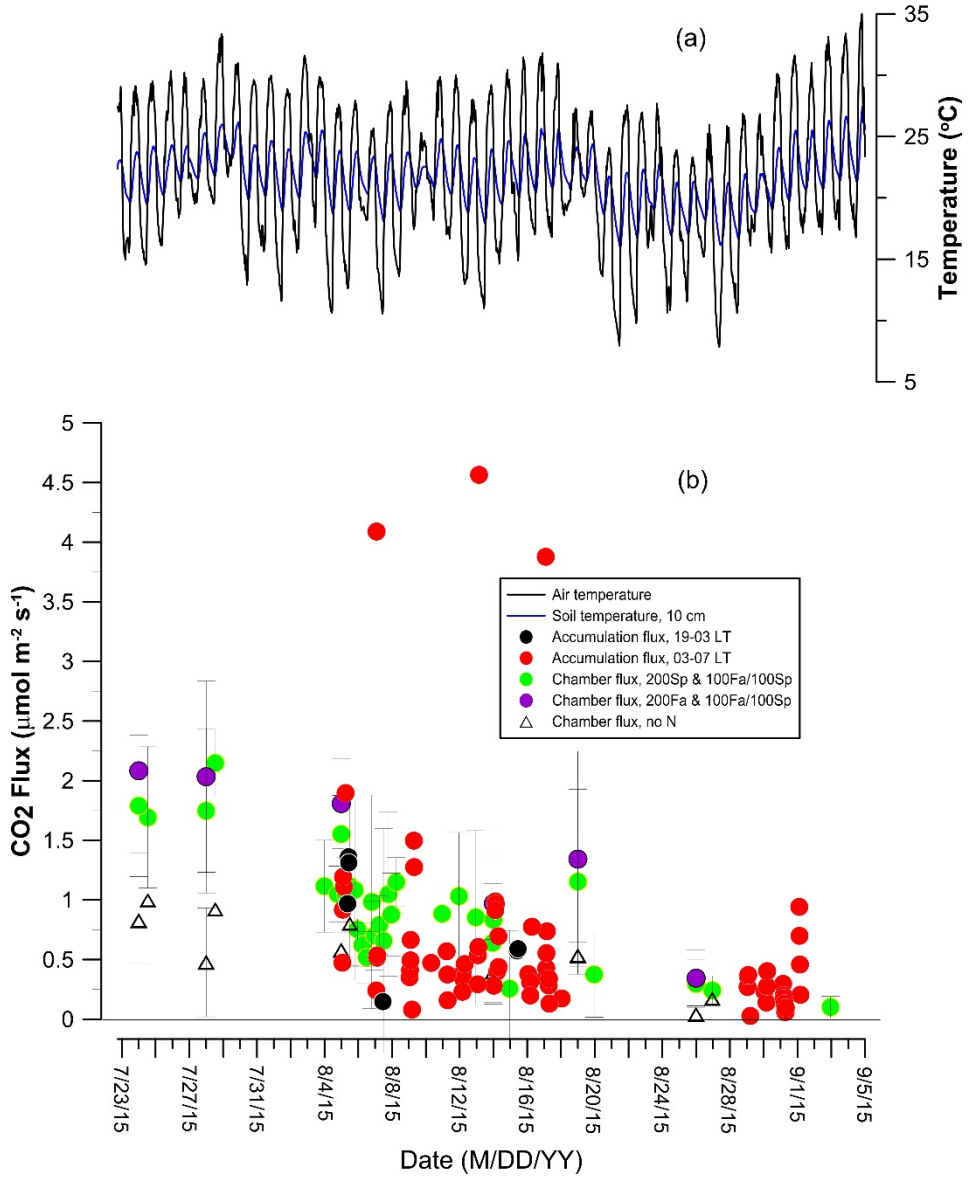

Figure 7: Temperatures and CO_2 flux based on accumulation and chamber methods. Diurnal variation in air (solid black line) and 10 cm soil at 10 cm depth (dashed blue line) during the period are indicated in panel a. Total fluxes (accumulative within and diffusive out the top of the control volume) under stable, low turbulence conditions and soil+root fluxes calculated using the chamber method are indicated in panel b (ordinate axis with differing units to left and right). The standard deviation of the three chamber flux measurements in each field are indicated by the vertical bars.

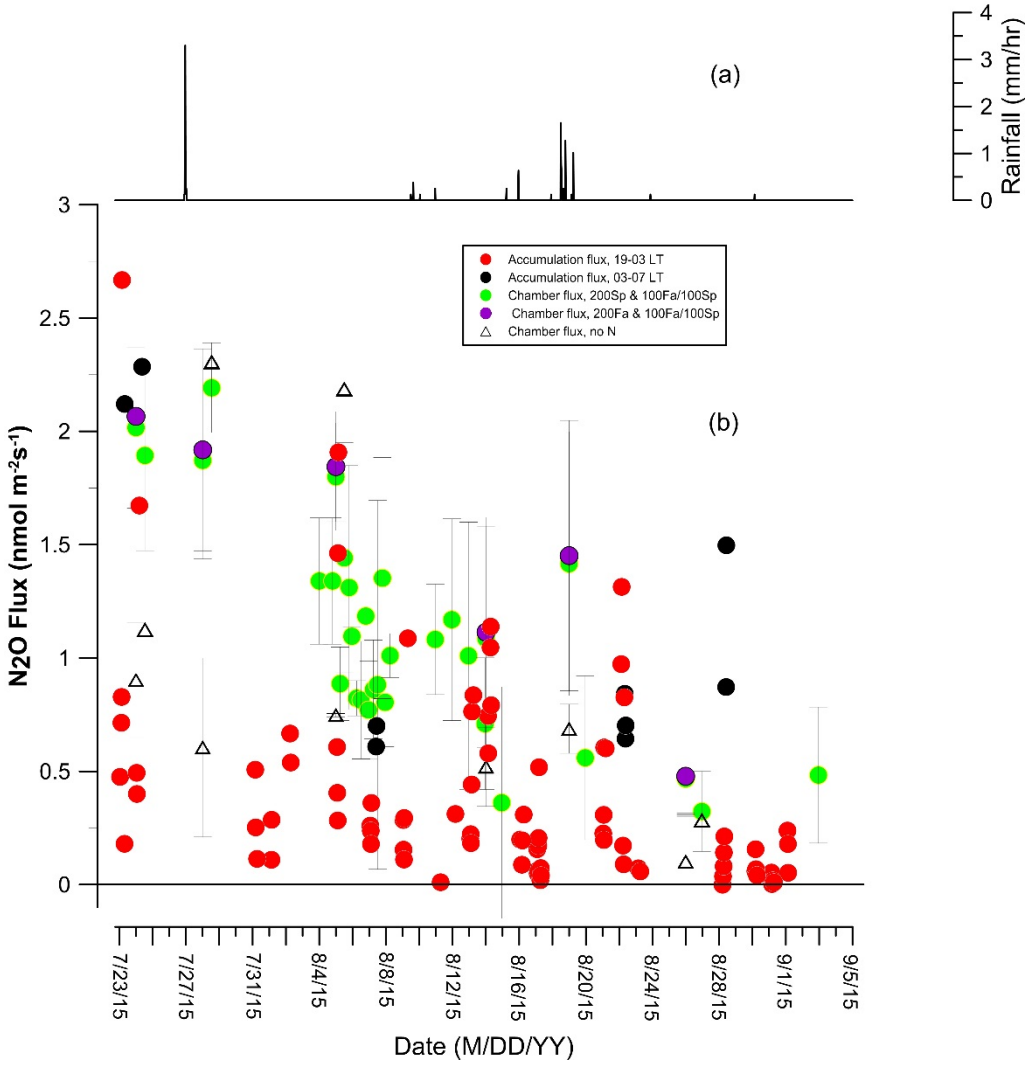

Figure 8: Precipitation and N_2O flux based on accumulation and chamber methods. Precipitation is indicated in panel a. Total fluxes (accumulative within and diffusive out the top of the control volume) under stable, low turbulence conditions and soil+root fluxes calculated using the chamber method are indicated in panel b (ordinate axis with differing units to left and right). The standard deviation of the three chamber flux measurements in each field are indicated by the vertical bars.